Durability of Reinforced Concrete Beams Externally Strengthened with CFRP Laminates under Harsh Climatic Conditions

Nasser Al Nuaimi, Ph.D.[1]; Muazzam Ghous Sohail, Ph.D., M.ASCE[2]; Rami Hawileh, Ph.D., M.ASCE[3]; Jamal A. Abdalla, Ph.D., F.ASCE[4]; and Kais Douier[5]

Abstract: This paper addresses the durability of reinforced concrete beams strengthened with carbon fiber-reinforced polymer (CFRP) laminates under natural and saline environments in the Arabian Gulf. Beam specimens were conditioned under sunlight and saline water for 180, 360, and 730 days and tested under four-point bending until failure. The load–deflection curves, strains, failure modes, ductility, and stiffness of the exposed beams were evaluated. The CFRP-strengthened specimens exhibited a 67% higher ultimate load capacity than control specimens after 28 days and up to 51% and 71% higher load capacity than control specimens after two years of direct sunlight and saline water exposure, respectively. No pronounced loss in strength and stiffness or damage to the epoxy was observed. Failure modes were transformed from cohesive to adhesive due to saline water exposure, whereas sunlight-exposed samples exhibited no failure-pattern change, and failures remained cohesive or interfacial. For design and analysis, environmental strength reduction factors are proposed and compared to current industry guidelines. Thus, CFRP-strengthened laminates can endure and perform effectively when subjected to severe environments of high salinity, temperature, and humidity. **DOI: 10.1061/(ASCE)CC.1943-5614.0001113**.

Author keywords: Durability; CFRP; Rehabilitation; Infrastructure strengthening; Reinforced concrete beams; Epoxy.

Introduction

Carbon fiber-reinforced polymers (CFRPs) are the most frequently used materials for the strengthening and rehabilitation of reinforced concrete (RC) structures due to their positive attributes, such as being lightweight and corrosion resistant, and having high tensile strength (Bakis et al. 2002; Gamage et al. 2005; Hawileh et al. 2011; Naser et al. 2012, 2019; Salama et al. 2019). Mechanical properties, such as the flexural, shear, and axial strength, of RC members are enhanced significantly with CFRP-based strengthening systems (Bahn and Harichandran 2008; Al-Tamimi et al. 2011; Shehata et al. 2011). However, the long-term durability of CFRP systems when subjected to the harsh conditions of high temperature, humidity, and saline water must still be investigated to better understand the degradation mechanism (Karbhari et al. 2003; Smith et al. 2005; Helbling et al. 2006; Choi et al. 2012; Chotickai and Somana 2018). The major concerns are the response of fiber-reinforced polymers (FRPs), the bond between the FRP composites and concrete interface, and the durability of the entire strengthened element during service life under severe conditions (Karbhari and Zhao 1997; Smith et al. 2005).

A committee of researchers (Karbhari 2003) that formed to identify the knowledge gap concerning the long-term performance of FRP materials argued that, as far as durability is concerned, the data are scarce, which causes concern regarding their use among the engineering and research communities. Moreover, the limited available data also reveal contradictory conclusions about the durability performance of epoxy-based composite materials. For instance, Al-Tamimi et al. (2011) reported a gain in strength in the CFRP-strengthened prism samples conditioned under saline water and sunlight exposure for two years. Hanna and Jones (1997) observed that the FRP-wrapped specimens showed no loss in strength, with no change in strain behavior, under moisture and temperature exposure for 40 and 140 days. Tatar and Hamilton (2016a) analyzed the degradation indices from selected literature and observed that either a complete loss of strength occurs with degradation indices equal to zero, or a gain of strength of up to twice the control strength occurs. Therefore, extensive applications of FRP–epoxy-based materials in the repair and strengthening of RC structures are still inhibited.

Two of the main critical identified areas, where a lack of reliable data exist to generate conclusive evidence regarding the durability performance of FRPs, are the performance of CFRP systems under direct sunlight and saline water exposure (Karbhari 2003; Karbhari et al. 2003; Al-Tamimi et al. 2015; Micelli et al. 2015; Sen 2015; Tatar and Hamilton 2016a; Liu et al. 2019). Dolan et al. (2009) investigated the durability performance of CFRP systems under 12 different environments. The most critical conditions, where degradation is severe and rapid, were observed to be immersion underwater at high

[1]Director, Center for Advanced Materials, Qatar Univ., P.O. Box 2713, Doha, Qatar. Email: anasser@qu.edu.qa

[2]Postdoctoral Research Fellow, Center for Advanced Materials, Qatar Univ., P.O. Box 2713, Doha, Qatar (corresponding author). ORCID: https://orcid.org/0000-0002-1826-2741. Email: muazzam.ghous@qu.edu.qa

[3]Professor, Dept. of Civil Engineering, American Univ. of Sharjah, P.O. Box 26666, Sharjah, United Arab Emirates. Email: rhaweeleh@aus.edu

[4]Professor, Dept. of Civil Engineering, American Univ. of Sharjah, P.O. Box 26666, Sharjah, United Arab Emirates. Email: jabdallah@aus.edu

[5]Research Associate, Dept. of Civil Engineering, American Univ. of Sharjah, P.O. Box 26666, Sharjah, United Arab Emirates. Email: kdouier@aus.edu

Note. This manuscript was submitted on June 5, 2020; approved on November 18, 2020; published online on January 21, 2021. Discussion period open until June 21, 2021; separate discussions must be submitted for individual papers. This paper is part of the ***Journal of Composites for Construction***, © ASCE, ISSN 1090-0268.

temperatures and exposure to humidity (no accumulation of water at the FRP interface) with elevated temperatures.

In certain regions, the temperature reaches up to 50°C, which results in a concrete surface temperature of above 60°C to 70°C, which is in the range of the glass transition temperature (T_g) of most commercially available epoxy adhesives. Epoxy adhesives lose tensile strength and modulus when heated up to T_g (Myers et al. 2001; Gamage et al. 2005). The moisture ingress also negatively affects cross-linking in the epoxy matrix, damages CFRP laminates and fibers, and weakens the interfacial bond between the epoxy and concrete substrate. The fiber-matrix interface is also damaged under moisture exposure (Myers et al. 2001; Helbling et al. 2006; Tatar and Hamilton 2016b, c; Tatar et al. 2016; Liu et al. 2019). Myers et al. (2001) reported an up to 60% stiffness loss in beams strengthened with CFRP when applied to the temperature and humidity cycles. Helbling et al. (2006) observed that, with the applied strain at high temperatures, the moisture intake by the FRP matrix increased. In addition, after 18 months of hygrothermal exposure, the localized damage and defects in the fibers become more pronounced.

The durability performance of concrete members strengthened with FRP sheets with different epoxy adhesives has also been investigated by researchers (Toutanji and Gómez 1997; Grace and Singh 2005; Choi et al. 2012; Tatar and Hamilton 2016a). Choi et al. (2012) studied the durability of three epoxy systems and two types of CFRP sheets. Strengthened prism specimens were conditioned under different environmental conditions, such as alkaline solution, saline water, ultraviolet (UV) light, outdoor exposure, and hygrothermal exposure from 30°C to 60°C, for 18 months. Different ratios of resin and hardener were tested. The main conclusion was that all adhesive systems respond differently to applied environmental conditions. The mixing ratio, resin type, and applied amount affect the durability of CFRP-strengthened systems at the level of the interface and interlaminated fibers. Grace and Singh (2005) tested the durability of RC beams strengthened with CFRP fabrics and CFRP plates under 100% humidity, salinity, alkalinity, and cyclic loading. It was observed that 100% humidity conditions had more pronounced effects on CFRP plates than on CFRP fabrics. However, the 100% humidity and saline water exposure caused a slight enhancement in the load-carrying capacity for CFRP fabrics.

Toutanji and Gómez (1997) reported the performance of three types of epoxies, two types of CFRP sheets, and two glass fiber-reinforced polymers (GFRPs) sheets, bonded to $51 \times 51 \times 356$ mm beams in flexure after wet/dry cycles in saline water. Epoxy adhesives and their bond with the concrete substrate were the most critical factors in the durability of strengthening systems under applied harsh climatic conditions. Polyoxypropylenediamine (hardener/epoxy resin) epoxy systems performed better than two systems, which were the modified amine/epoxy-resin blend and the 50% bisphenol-A epoxy resin with 25% polyoxypropylenediamine systems. Both types of CFRP sheets performed better than GFRPs under all types of exposure.

El-Hawary et al. (1998, 2000) tested epoxy-strengthened concrete cylindrical samples and shear slant samples under saline, open-air, and laboratory environments. The samples were broken and repaired with three epoxy types and were exposed to these environments for 6, 12, and 18 months. It was observed that, after an initial loss of strength, there was a regain, which is attributed to the seasonal temperature and humidity effects. The results indicated that the type of epoxy plays a vital role in the strength of concrete specimens under saline, open, and laboratory conditions.

Pan et al. (2015) investigated the effect of water immersion on the mechanical performance of CFRP systems in the single-lap shear test. The effects of immersion time (0, 2, 4, 6, and 8 weeks), the thickness of the applied epoxy layer (0.20 and 1 mm), and two different temperatures (20°C and 50°C) were investigated. Water uptake increases with the immersion time and higher temperatures. After eight weeks of immersion at 20°C, the modulus of elasticity was reduced by 1%, whereas the tensile strength was reduced by 6%. At 50°C, the reduction was 14.4% and 8.5%, respectively. The failure modes in single-lap shear tests changed from cohesive (concrete fracture) to adhesive (debonding of the sheet from the substrate) after two weeks of exposure to water at both temperatures. Li et al. (2019) conducted an extensive literature review on the durability performance of FRP–epoxy systems exposed to the saline environment. The epoxy adhesives degrade when the concentration of sodium chloride (NaCl) increases. Epoxy loses its strength rapidly under a high concentration of NaCl. Higher temperatures and lengths of exposure time also degrade the epoxy.

Nishizaki et al. (2005) presented the results of five years of conditioning of two CFPR systems (A and B) under three natural environments; two places were in Japan (Okinawa and Tsukuba), and one was in Canada (Sherbrook). The study was intended to be 10 years long. The presented results were at the half-way point of the study and addressed degradation after 0, 1, 3, and 5 years. The tensile strength of the CFRP was slightly reduced after one and three years; however, it recovered at five years and reached 0.88 and 1 times the initial strength. In a review, Sen (2015) summarized the results of this study after 10 years, and no significant degradation was observed in the tensile strength of the two tested CFRP systems. However, the modulus of elasticity reduced by 20% for System A, whereas a much smaller reduction was found for System B. Sen (2015) presented a review of the long-term durability performance of CFRP systems in real-time application and laboratory studies. They reported that the structures that were strengthened with CFRP are still in service after 30 years and are apparently in good condition, without showing any loss in strength. Al Azzawi et al. (2018) reported the performance of CFRP-strengthened concrete masonry unit walls under the hot and humid climate of Florida, USA. The bond between the CFRP and masonry units was not degraded over 20 years, whereas no repair coat was provided during that time, and such a repair system is deemed durable.

Studies have suggested that the interfacial bond between FRP and concrete substrates is more severely damaged under the synergic effects of a harsh climate and applied loading (Myers et al. 2001; Gamage et al. 2005; Abbas 2010; Cabral-Fonseca et al. 2011; Al-Tamimi et al. 2015). However, small prisms and single-lap shear test samples were investigated in these studies. The durability of typical-scale beams has not been extensively studied. Concluding the status of the research and findings regarding the durability of FRP–epoxy systems, temperature and moisture have adverse effects on the bond strength, tensile strength, and modulus of elasticity of FRP–epoxy systems. Especially the moisture ingress could initiate the plasticization of the epoxy matrix and reduce its strength. However, different FRPs and epoxy systems responded differently to the applied conditions (Dolan et al. 2009; Li et al. 2020).

This study aims to evaluate the durability performance of CFRP-strengthened RC beam under the harsh natural environment of Qatar and similar regions, where sustained sunlight, saline water, and airborne chlorides are encountered. Specimens were exposed to laboratory conditions, outdoor sunlight, and immersion underwater with 3% NaCl for a period of 6, 12, and 24 months. The environmental strength reduction factors (C_E) for the exposed CFRP beams were established based on strength retention in comparison with the unstrengthened and unexposed specimens, controlled and strengthened laboratory specimens, and control (unstrengthened)

specimens exposed to the same environment during the same period. According to the authors' knowledge, such a thorough comparison of the typical-scale CFRP-strengthened RC beams had not been extensively studied for long-term durability under real-time harsh climates. For the design and analysis of CFRP-strengthened beams, the strength reduction factors (C_E) are recommended based on the results of this study and compared with those recommended by American Concrete Institute (ACI) 440.2R-17 (ACI 2017) guidelines. The study is expected to enhance the confidence in the use of CFRP strengthening and minimize concerns regarding their performance under harsh climatic conditions.

Experimental Details

Sample Geometry and Testing Matrix

Forty typical-scale RC beams were cast. Fig. 1 depicts the specimen dimensions and reinforcement details. The length of each beam was 2 m, and the cross-sectional dimensions were 140 × 280 mm. The beam samples were designed as a tension-controlled section per ACI Committee 318 (ACI 2014) flexural design guidelines. An adequate number of stirrups were provided to avoid shear failure. This helps clarify the effect of the conditioning on the contribution of CFRP strengthening. The primary flexural reinforcement consisted of two bars that were 12 mm in diameter, and the top compression reinforcement was two bars that were 8 mm in diameter. Stirrups of 8 mm-diameter rebar were provided at a distance of 120 mm center-to-center in the shear spans, and the distance between the central two stirrups was 100 mm, as illustrated in Fig. 1. Fig. 1 also schematically presents the final layout of the strengthened specimens. The CFRP sheets were placed over a length of 1,600 mm, whereas 200 mm from either side was left uncovered. The width of CFRP laminates was 100 mm; hence, 20 mm of beam width from either side of the sheets was not strengthened. The thickness of the CFRP sheet was 0.17 mm, and the final thickness of the CFRP laminates (CFRP plus epoxy) was estimated to be 1.02 mm.

Table 1 presents the testing plan for the RC beam specimens. The samples were divided into three main categories, depending on the exposure type: laboratory conditions, outdoor sunlight, and immersion in saline water. Each group was subdivided into three further groups, depending on the exposure period (i.e., 6, 12, and 24 months). For each set of exposure type, two CFRP-strengthened and two control specimens were cast. This was to eliminate possible error in workmanship and material variability while obtaining reliable results. The number of samples was limited to two because these beams samples are not easy to handle and control in large numbers, which would be the case if the samples for each category were increased to three. In addition, two samples each were also tested at 28 days to establish a benchmark to study the effects of exposure and time on the strengthened RC beams. The specimens were designated according to their exposure type and time of testing. For instance, for the CB-S-180-1 specimen, CB stands for control beam, S denotes sunlight exposure, 180 represents the length of exposure in days, and 1 indicates that it is the first beam to be tested in this category. Moreover, C-360-W-2 represents a CFRP-strengthened beam exposed to saline water (W) for 360 days, which is the second beam to be tested in this category.

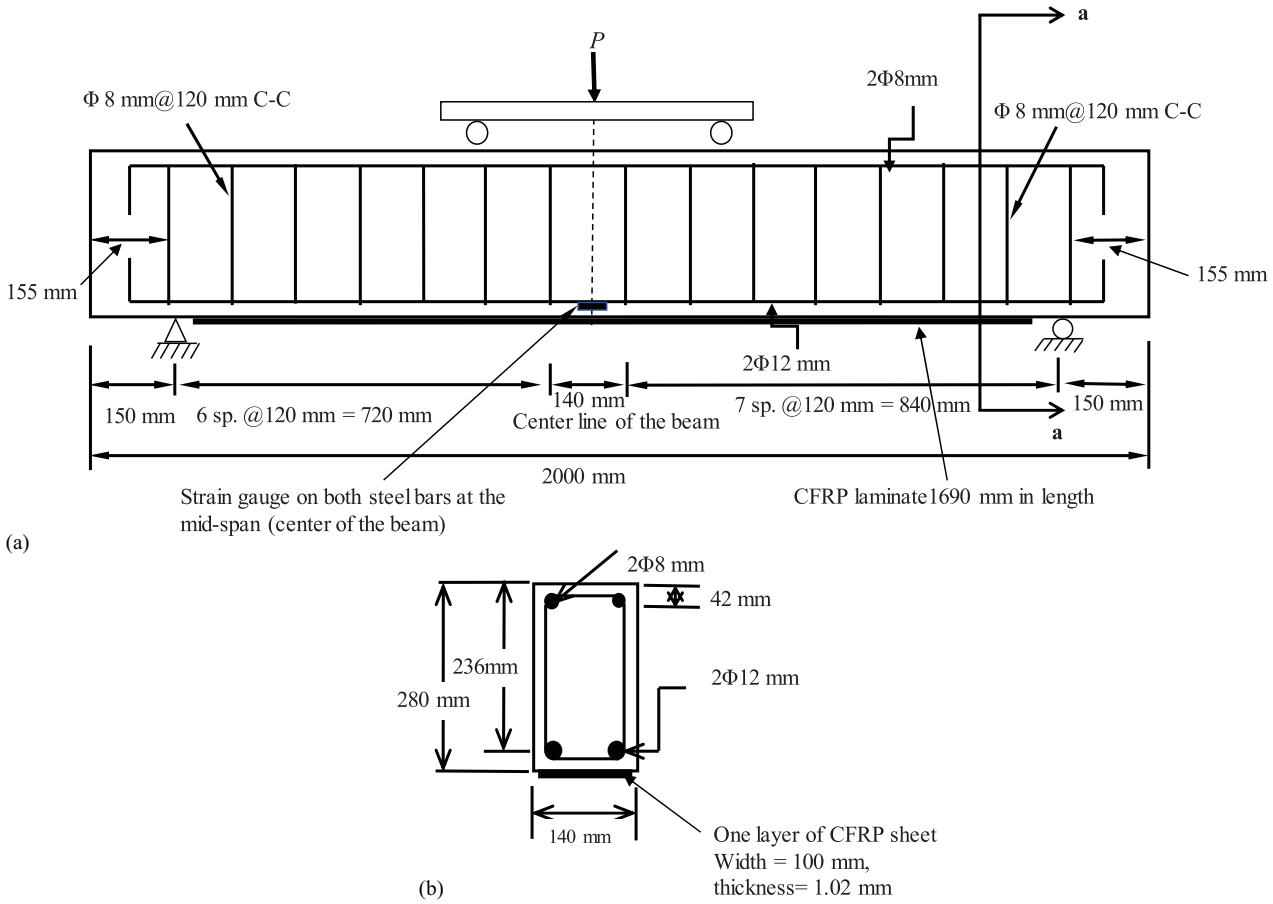

Fig. 1. Dimensions of typical-scaled concrete beams with reinforcement detail: (a) front view; and (b) cross-sectional view.

Material Properties

Concrete

All the beam specimens were cast with one concrete batch of a target compressive strength of 40 MPa. The locally produced Ordinary Portland Cement CEM I R42.5, Gabbro coarse aggregates with a size range of 12.5–19.5 mm, and washed sand with a size range of 0 to 4.75 mm, were used as the concrete ingredients. The measured slump of concrete as per the American Society for Testing Materials (ASTM) C143/C143M-15a (ASTM 2015) was 180 mm. The compressive strength was measured on six cylindrical concrete samples of 150 × 300 mm dimensions after 28 days of curing following ASTM C39/C39M-17 (ASTM 2017). The average, minimum, and maximum values of compressive strength were 45, 44, and 47 MPa, respectively, with a standard deviation of 1.03. The flexure tensile strength was measured per ASTM C1609/C1609M-12 (ASTM 2012) on six prisms of 150 × 150 × 550 mm. The average, minimum, and maximum values were 4.5, 3.7, and 5.2 MPa, respectively, whereas the standard deviation was 0.59.

Steel Rebar

The main flexure reinforcement, compression reinforcement, and stirrups were of deformed mild carbon steel rebar conforming to ASTM A615/A615M-16 (ASTM 2016). The average yield strength measured on the three samples was 560 MPa, whereas the average ultimate strength was 600 MPa. The modulus of elasticity was 200 GPa. The reinforcement detail is depicted in Fig. 1.

Table 1. Testing matrix of strengthened and unstrengthened carbon fiber reinforced polymer (CFRP) control beams

	Exposure					
	Laboratory		Sunlight		Saline water	
Exposure duration	CB	CFRP	CB	CFRP	CB	CFRP
28 days	2	2	—	—	—	—
6 months	2	2	2	2	2	2
12 months	2	2	2	2	2	2
24 months	2	2	2	2	2	2
Total = 40 beams	8	8	6	6	6	6

Carbon Fiber-Reinforced Polymer Laminates (Sheets and Epoxy)

In this study, commercially available CFRP laminates (V-Wrap™ C200H 2014) were employed. As per the manufacturer, the CFPR laminates (sheet with epoxy) had a design thickness of 1.02 mm, tensile strength of 1,240 MPa, modulus of elasticity of 73.8 GPa, and strain at rupture of 1.7%. The CFRP sheets were attached to concrete surfaces using a two-component epoxy comprising Parts A (epoxy) and B (hardener) (V-Wrap™ 700S 2014). As per the instructions of the manufacturer, Part A was premixed for 2 min, and then the entire packaged quantities of both parts were mixed for 3 min at about 400 rpm. Because the epoxy resin has an immense influence on the durability properties of strengthened materials, it is important to mention the properties of the epoxy system. The epoxy had a modulus of elasticity of 3.2 GPa, tensile strength of 45 MPa, and elongation at rupture of 5.5%. The T_g of this epoxy adhesive was 76.6°C.

Strengthening Application Procedure

Soffits of the beams were sandblasted to have a roughened concrete surface for CRFP laminate application, as illustrated in Fig. 2. The wet-layup method was used, in which the CFRP sheets were first immersed in a prepared epoxy until saturation was achieved. First, a layer of epoxy adhesive was applied at the prepared concrete surface [Fig. 2(a)]. Then, the saturated laminates were carefully placed at the marked length of the beam soffit [Fig. 2(b)], followed by another epoxy layer applied at the top surface of the sheets [Fig. 2(c)]. Steel rollers were moved with gentle pressure over the sheets to remove all air voids. The strengthening procedure was conducted after curing the concrete beams for two weeks. After application, the epoxy adhesives cured for two more weeks for the specimens tested at 28 days.

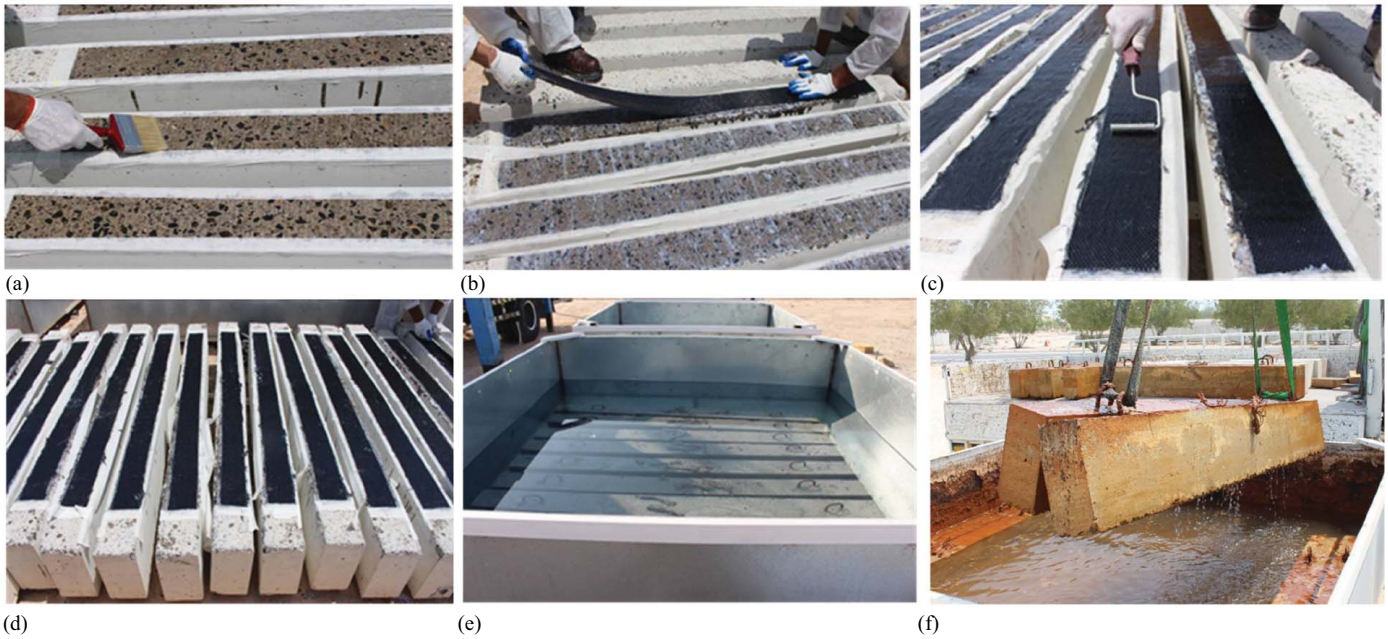

Fig. 2. Strengthening procedure: (a) surface preparation; (b) application of carbon fiber-reinforcement polymer (CFRP) laminates; (c) epoxy coat on the CFRP laminates; (d) sunlight exposure; and (e and f) immersion under saline water.

Environmental Conditioning

After strengthening, the beams were exposed to sustained sunlight [as shown in Fig. 2(d)] and immersed under saline water with 3.5% NaCl [Figs. 2(e and f)]. In contrast, the laboratory conditioned specimens were placed inside a room with a controlled climate of temperature 23°C and relative humidity (RH) of about 40%. The exposure of the specimens was carried out in the facilities of the Qatar University in Doha, Qatar. It was an open area with no shelter for the sunlight-exposed samples. Saline water tanks were also directly exposed to sunlight, and the tanks were refilled regularly to keep the sample immersed for up to two years. The climate in Doha city is extreme, with temperatures between 18°C and 50°C and RH between 40% and 100%. The UV index varies from 6 in January to 12 in the months of June to October. From May to October, the temperature remains in the range of 40°C to 50°C, and the RH is between 80% and 100%.

Instrumentation and Experimental Setup

Fig. 3 presents the instrumentation for the four-point bending tests performed using a servo-hydraulic test frame with a load capacity of 2,000 kN. Displacement control loading was applied at a rate of 1 mm/min. The machine support rollers provided the conditions of a simply supported beam. The tested span length was 1,690 mm between the two reaction supports, and the shear span was 561.5 mm, the distance between the reaction support and loading point. The loading points at the top of the beams were 567 mm apart. A strain gage was applied at each flexural reinforcement at the top surface of the beam and the bottom of the CFRP laminates, all at the midspan of the beam. Two L-shaped aluminum rods were pasted at either side of the beam at midspan, and linear variable displacement transducers were fixed to them to measure the deflections, as displayed in Fig. 3.

The loads versus deflections and strain curves were recorded through the data acquisition machine. Furthermore, the crack initiation and propagation in the beams and possible debonding or fiber rupture in the CFRP laminates were visually monitored.

Degradation Factors and Ductility Indices

The effects of the exposure types and their application times were assessed in terms of strength retention by the CFRP-strengthened RC beams. The parameters (degradation factors) used to analyze the results are elaborated in Eqs. (1)–(5). These strength reduction factors are developed based on the approach presented by Tatar and Hamilton (2016c). Fig. 4 schematically explains the concept behind these degradation factors. Measuring the loss in flexural strength and bond strength through ultimate loads after exposure is an indirect method to evaluate the environmental effects on the durability of the FRP–epoxy strengthening systems. The laboratory strength ratio (*LSR*) was used to quantify the gain in strength with a CFRP-strengthened system. It is the ratio between the ultimate load capacity of the strengthened laboratory specimen, P_{nf}, divided by the ultimate load of the control-laboratory specimen, P_{nl}, as shown in Eq. (1). The exposure strength ratio (*ESR*) is obtained by dividing the ultimate load of a strengthened exposed specimen, P_{nfe}, to the ultimate load of an unexposed strengthened laboratory specimen, P_{nf}. This factor covers the possible degradation of the concrete matrix, steel corrosion, damage to FRP materials, and degradation of epoxy adhesives under certain exposure types and times.

To assess the bond strength retention, the degradation originated from the concrete member (corrosion or concrete decay) must be subtracted, and only the degradation on the level of epoxy adhesives is considered. For this purpose, indices R_b and R_{b28} are introduced [Eqs. (3) and (4)], where the original strength of the exposed concrete member, P_{ne} is subtracted from the total strength of the strengthened exposed CFRP beams, P_{nfe}, and the strength of the unexposed concrete member, P_{nl} , is subtracted from the total strength of the unexposed CFRP-strengthened member, P_{nf}. For further clarification, please refer to Fig. 4. For R_b, the difference $(P_{nfe} - P_{ne})$ was divided by $P_{nf} - P_{nl}$, which quantifies the bond degradation. Similarly, the bond degradation against 28-day samples was calculated by R_{b28}. The flexure strength retention factor, R_n, is elaborated in Eq. (5), and the ultimate strength of an exposed-strengthened specimen is divided by the ultimate strength of an unexposed strengthened specimen; this value is further divided by the ratio of strength between the exposed unstrengthened to unexposed unstrengthened values [Eq. (5)]:

$$LSR = \frac{P_{nf}}{P_{nl}} \tag{1}$$

$$ESR = \frac{P_{nfe}}{P_{nf}} \tag{2}$$

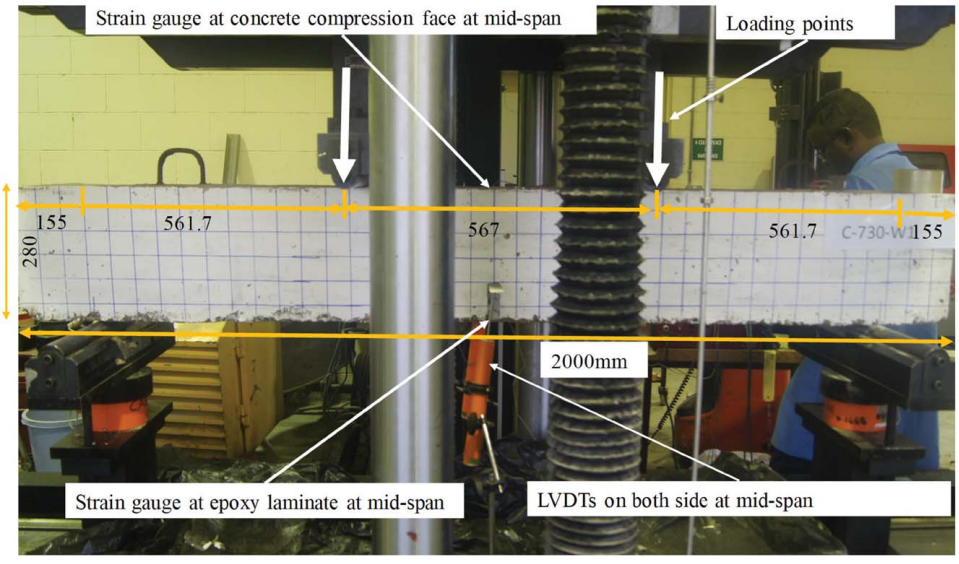

Fig. 3. Testing setup for RC beams strengthened in flexure. All dimensions are in millimeters.

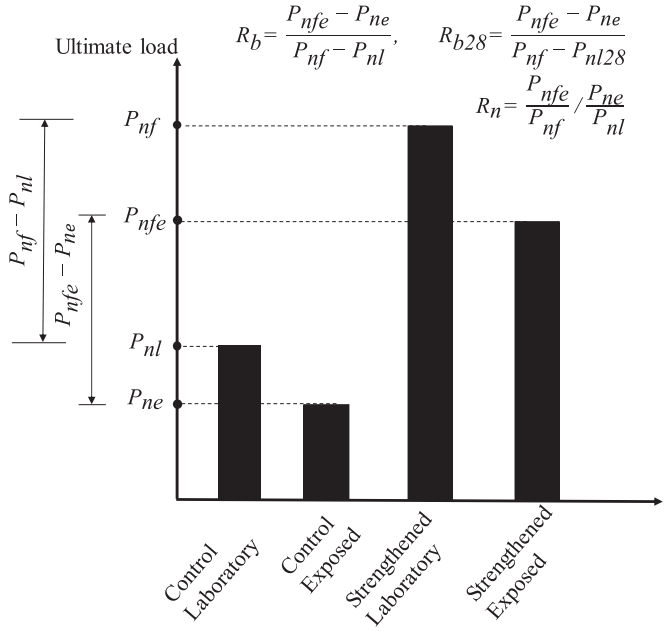

Fig. 4. Schematic diagram explaining the degradation factors based on the load-carrying capacity. (Adapted from Tatar and Hamilton 2016a.)

$$R_b = \frac{P_{nfe} - P_{ne}}{P_{nf} - P_{nl}} \tag{3}$$

$$R_{b28} = \frac{P_{nfe} - P_{ne}}{P_{nf} - P_{nl28}} \tag{4}$$

$$R_n = \frac{P_{nfe}}{P_{nf}} / \frac{P_{ne}}{P_{nl}} \tag{5}$$

where P_{nl}, P_{nf}, P_{ne}, and P_{nfe}, = ultimate loads of the control laboratory specimen, strengthened laboratory specimen, exposed control specimen, and exposed strengthened specimen, respectively.

Two parameters were defined for the beam ductility until the yielding of the main reinforcement and after reaching the ultimate loads. Eqs. (6) and (7) elaborate these ductility indices, respectively:

$$\mu_{\Delta y} = \delta f / \delta y \tag{6}$$

$$\mu_{\Delta u} = \delta f / \delta u \tag{7}$$

where δy, δu, and δf = deflection at the steel yielding, ultimate load, and failure loads, respectively.

Results and Discussion

The durability of CFRP-strengthened RC beams under sunlight and saline water exposure for 6, 12, and 24 months was assessed based on their residual strengths. The results were evaluated through failure modes under four-point bending, crack initiation, load versus deflection curves, overall beam stiffness, yield and ultimate loads, and their respective deflections. The following are the results after each exposure period.

Failure Modes

Fig. 5 lists the failure modes in CB and CFRP-strengthened specimens at 28 and 180 days, and Fig. 6 lists the failures after 360 and 730 days of laboratory, sunlight, and saline water exposure. One sample from each category was selected to demonstrate the effect of conditioning on the type of failures in the CFRP beams. However, the failure modes of each specimen are presented in Table 2. In the case of CFRP-strengthened beam specimens, up to four types of failure modes were observed: cohesive, adhesive, interfacial, and rupture of laminates. Cohesive failure is primarily in the concrete matrix near the tensile face, where a large chunk of concrete is delaminated from the bulk, and the bond between the concrete layer and laminates is not broken. Interfacial failure is a mix with the debonding of laminates from some part of the concrete surface with failure also passing through the concrete cover. Adhesive failure is on the level of the bond at the interface between the composites and concrete substrate. Only the CFRP laminates debond from the soffit of the beams with some traces of concrete on the surface. The rupture of CFRP laminates at failure is considerably rare in the case of concrete application. These failure modes have been observed and reported in several studies in the literature (Grace and Singh 2005; Choi et al. 2012, Hawileh et al. 2014; Tatar and Hamilton 2016c; Choobbor et al. 2019). In this study, the first three types of failure were observed in the beams tested at 28 days and up to 730 days of applied exposure (Figs. 5 and 6).

The failure in CBs was a conventional one under all exposure types. At first, flexural cracks appeared, then the yielding of the flexural reinforcement initiated, followed by concrete crushing under compression [Fig. 5(a)]. In CFRP-strengthened specimens, the failure was initiated with the appearance of flexural cracks, followed by steel yielding, shear cracks, debonding or delamination, and then concrete crushing at the top compression face. First, flexural cracks appeared and moved along the epoxy at the interface between the CFRP laminates and concrete surface, which resulted in either cover separation or sheet debonding. The case in which epoxy adhesives resisted higher loads, higher stress concentrations occurred at the laminate ends, which the concrete could not withstand, resulting in forming horizontal shear cracks and concrete delamination (concrete cover separation) causing cohesive failure.

From two samples tested at 28 days, one showed cohesive failure and the other exhibited interfacial failure with a large chunk of concrete cover attached to the CFRP laminate [Fig. 5(b)]. One sample tested at 180 days after laboratory exposure exhibited adhesive failure and the other exhibited interfacial failure. Both specimens that were exposed to saline water for 180 days had adhesive failures [Fig. 5(d)] with no concrete cover detached from the beam. Both samples that were exposed to the sunlight for 180 days had cohesive failures with the concrete cover separating from the level of the main reinforcement [Fig. 5(e)]. At 360 days, one cohesive [Fig. 6(a)] and one adhesive failure were observed in the laboratory specimens. All specimens exposed to the sunlight and saline water demonstrated adhesive failure [Figs. 6(b and c)]. At 730 days of exposure, the laboratory samples again exhibited the cohesive mode of failures, as it was the case for specimens tested at 28 days [Fig. 6(d)]. The sunlight-exposed specimens demonstrated cohesive and interfacial failure. Both samples exposed to saline water had adhesive failure with relatively concrete-free CFRP laminates. Although no clear pattern of failure mode with the time of exposure was found, the exposure type revealed that saline water transformed the failure mode from cohesive to completely adhesive starting from 180 days to 730 days. Laboratory exposure resulted in no change in failure mode, and most samples after 180, 360, and 730 days exhibited either cohesive or interfacial modes of failure. Sunlight exposure was

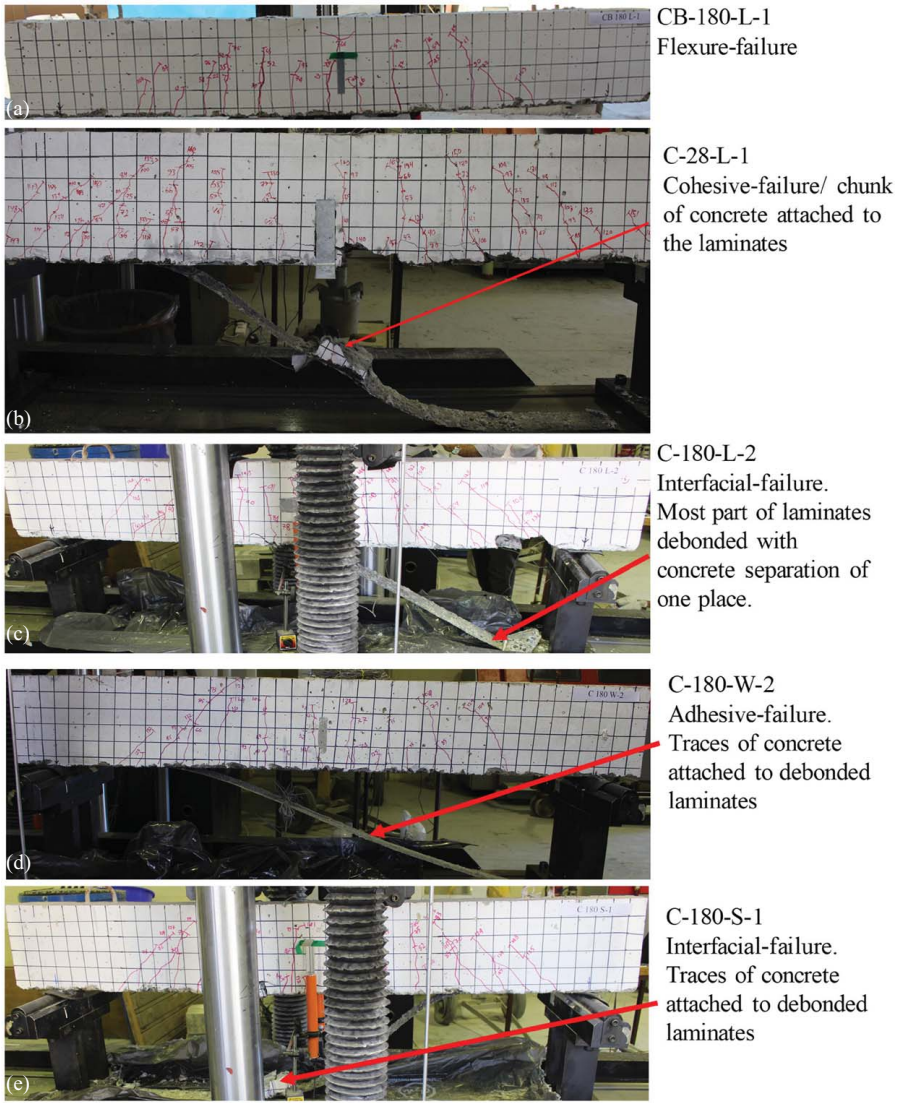

Fig. 5. Failure modes of control and carbon fiber-reinforced polymer (CFRP)-strengthened beams: (a) control beam; (b) CFRP at 28 days; (c) laboratory-exposed CFRP at 180 days; (d) saline water-exposed CFRP at 180 days; and (e) sunlight-exposed CFRP at 180 days.

also not as detrimental as the saline water exposure. This indicates that hydrothermal exposure is more severe than indoor and dry heat exposure. Pan et al. (2015) also reported a change in failure mode from cohesive to adhesive after only two weeks of water immersion on CFRP-strengthened single-lap shear samples. In contrast, Grace and Singh (2005) reported no change in failure mode for RC beams strengthened with CFRP fabrics and CFRP plates after 10,000 h of 100% humidity, in saltwater solution, and dry heat exposure. The observed failure mode was delamination or debonding of strengthening laminates.

The onset of debonding or concrete delamination primarily coincides with the ultimate load capacity of the beams, which means both occurred at the same loads, illustrating that the failures were initiated due to the debonding of the laminates or delamination of the concrete. Until failure, the concrete crushing at the compression zone was not initiated. However, as the sheet delaminated, concrete crushing immediately followed. This observation was made in all samples exposed for up to two years. This verifies that the CFRP laminates retain the integrity of the beam section until debonding and govern the failure load of the RC beam. The CFRP laminates or the individual carbon fibers were not broken or ruptured at failure.

Crack Initiation

In the RC beams, the cracks appear once the flexure stress crosses the modulus of rupture of concrete at the tension side of the beam. Because CFRP sheets provide confinement at the soffit of the beam and act as an external flexural reinforcement, resisting the applied moments, they increase the beam stiffness and its modulus of rupture to higher loads. In both CB and CFRP, vertical cracks appeared in the tension side in the constant moment area after a certain load level. The number of cracks increased and elongated in the compression zone. As loads increased, the cracks were also initiated in the shear zones on both sides. Once entered in the compression zone, all cracks became flexural-shear cracks and started to incline toward the loading points. This behavior was observed in all beams after all exposure types and times.

In the case of the CB, the cracks started appearing at between 21 and 33 kN loads, whereas in CFRP-strengthened specimens, they appeared at between 35 and 53 kN. That is a 66% to 152% increase in the load at the first crack. The exposure to sunlight and saline water for up to two years exhibited no effects on the crack loads. The exposure conditions did not reduce the ability of the CFRP-strengthened systems to delay crack initiation. The delay in the cracking load is

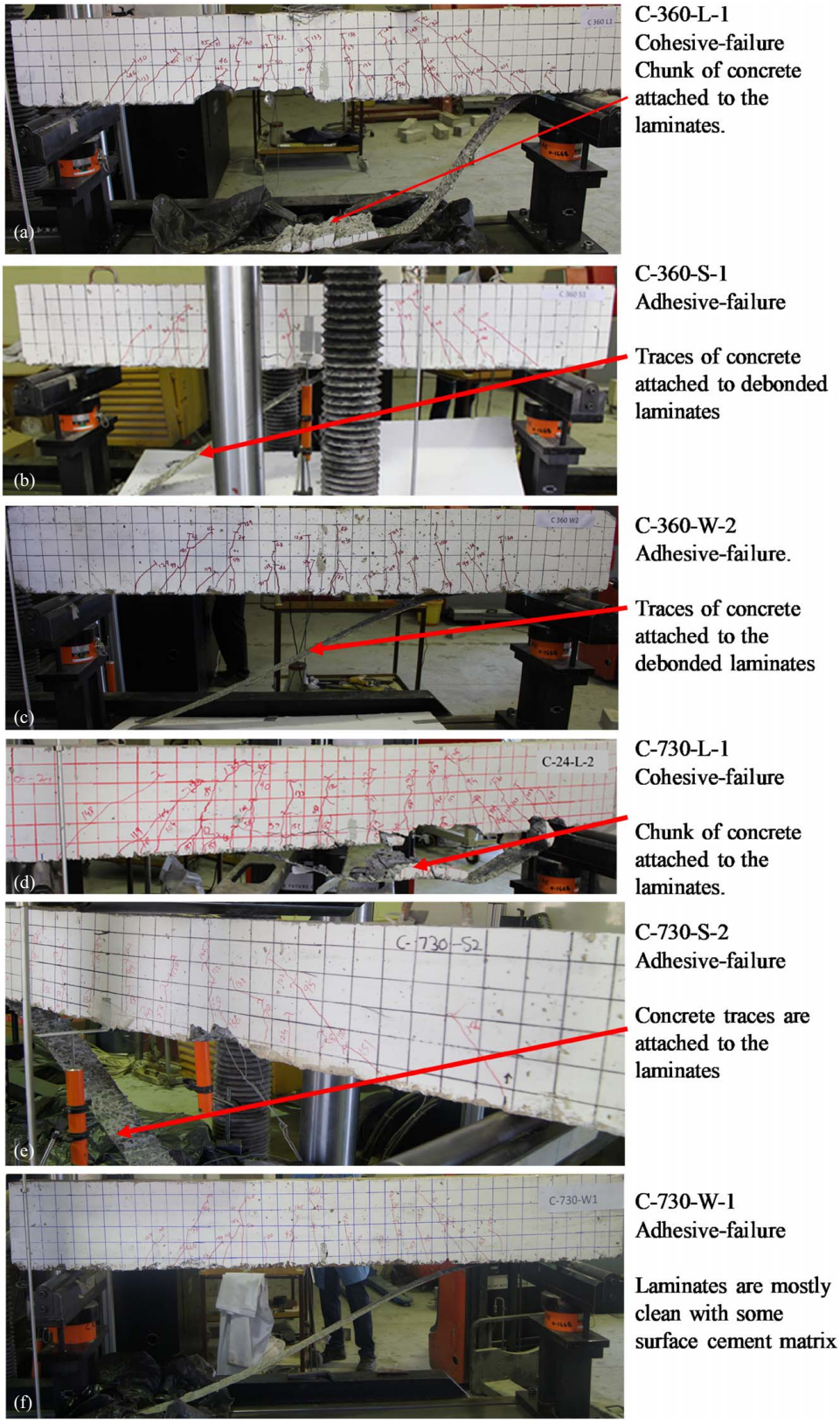

Fig. 6. Failure modes of carbon fiber-reinforced polymer (CFRP)-strengthened beam at 360 days of (a) laboratory; (b) sunlight; and (c) saline water exposure; and (d–f) CFRP after 730 days of laboratory, sunlight, and saline water exposure, respectively.

an essential aspect of the serviceability of RC structures because the cracks facilitate the ingress of harmful agents, such as chlorides and carbon dioxide to the steel surface. By minimizing the cracks at the service loads, the corrosion initiation can be retarded, which could positively affect the overall durability of the concrete structural members strengthened with CFRP.

The exposure conditions reduced the total number of cracks formed before failure in both the control and strengthened specimens.

Table 2. Summary of test results

Exposure time	Conditions	Str. Type	Loads/deflections							Ductility indices		Failure mode	
			P_y (kN)	P_u (kN)	% P_y incr.	% P_u Incr.	δ_y (mm)	δ_u (mm)	δ_f (mm)	δ_f/δ_y	δ_f/δ_u	1st sample	2nd sample
28 days	Lab	Control	89	90			8.5	10.2	10.4	1.23	1.02	Flexure	Flexure
		CFRP	124	150	40	67	9.2	15.5	15.7	1.70	1.01	Cohesive	Interfacial
6 months	Lab	Control	86	99			8.4	17.4	18.2	2.17	1.04	Flexure	Flexure
		CFRP	120	152	40	53	10.0	16.3	16.7	1.67	1.02	Adhesive	Interfacial
	Saline	Control	89	102			7.2	16.7	28.5	3.95	1.70	Flexure	Flexure
		CFRP	117	134	32	32	8.2	11.5	12.5	1.53	1.08	Adhesive	Adhesive
	Sun	Control	92	103			9.7	17.1	20.0	2.07	1.17	Flexure	Flexure
		CFRP	115	146	25	41	9.6	16.7	16.9	1.76	1.01	Cohesive	Cohesive
12 months	Lab	Control	89	101			8.0	16.8	17.9	2.24	1.06	Flexure	Flexure
		CFRP	122	150	38	49	8.7	14.6	15.2	1.76	1.05	Interfacial	Adhesive
	Saline	Control	91	99			7.3	13.9	15.0	2.07	1.08	Flexure	Flexure
		CFRP	120	141	33	42	7.2	11.7	12.3	1.71	1.06	Adhesive	Adhesive
	Sun	Control	91	99			8.4	16.4	16.7	2.00	1.02	Flexure	Flexure
		CFRP	119	147	30	48	8.7	14.8	15.2	1.76	1.03	Adhesive	Adhesive
24 months	Lab	Control	99	109			7.8	16.8	22.9	2.93	1.36	Flexure	Flexure
		CFRP	121	148	22	36	6.6	11.1	11.6	1.75	1.05	Cohesive	Interfacial
	Saline	Control	96	96			7.0	14.5	15.1	2.16	1.04	Flexure	Flexure
		CFRP	137	164	42	71	8.4	13.3	13.8	1.65	1.04	Adhesive	Adhesive
	Sun	Control	97	103			7.1	10.3	10.9	1.54	1.06	Flexure	Flexure
		CFRP	129	156	32	51	8.8	13.1	13.7	1.57	1.05	Cohesive	Interfacial

For example, the numbers of cracks at failure in CB-28-L- and CB-28-L-2 were 30 and 32, respectively. Moreover, in CB-360-S-1 and CB-360-S-2, the cracks numbered 24 and 18, respectively. In the strengthened specimens, such as C-28-L-1 and C-28-L-2, the numbers of cracks were 70 and 80, respectively. In the CFRP-strengthened specimens conditioned at the laboratory, the numbers of cracks in the two-beam specimens (Specimens 1 and 2) were 45 and 47 at 180 days, 48 and 40 at 360 days, and 47 and 46 after 730 days. For two beams under saline water, the numbers of cracks were 43 and 35, 31 and 33, and 41 and 31 after 180, 360, and 730 days of conditioning, respectively. After sunlight exposure, the numbers of cracks were 34 and 36, 33 and 34, and 49 and 47 for two samples tested at 180, 360, and 730 days, respectively. The decrease in cracks was higher for saline exposure than sunlight exposure. The laboratory specimens also exhibited a drop in cracks over time but not as much as in the other two outdoor exposure types. The CB specimens also demonstrated that the number of formed cracks at failure reduced from 32 to 21. The reduced number of cracks in CB could be due to the hydration of the unhydrated concrete, which might have enhanced the modulus of rupture of the concrete. In CFRP specimens, because the strength is increased over time in concrete and strengthening composites, the cracks reduced and the width of the cracks increased.

Load-Deflection Behavior

Fig. 7 illustrates the midspan load versus deflection curves for CB and CFRP-strengthened beam specimens tested at 28 days. Fig. 8 presents the curves for the samples tested at 180 and 360 days, and Fig. 9 presents the curves for the specimens tested after 730 days for all three conditions. The performance of CFRP-strengthened specimens was evaluated against the CB at 28 days, laboratory specimens at the same age, and CBs conditioned for the same periods. From the load versus deflection graphs, the beam stiffness, yield loads, ultimate loads, and deflections at steel yielding and beam failure were recorded. Table 2 presents their average values for the two specimens after 28 days of curing and after 180, 360, and 730 days of exposure.

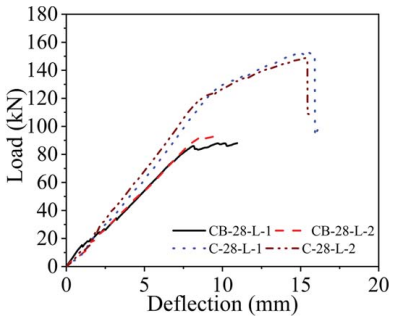

Fig. 7. Load–deflection curves for the control beam (CB) and carbon fiber-reinforced polymer (CFRP)-strengthened beam at 28 days of curing.

Figs. 7–9 reveal that the load–deflection curves were bilinear for CB and CFRP-strengthened specimens until failure. The initial low values due to the support and loading arm adjustments before the application of bending loads on the beams were filtered from all the curves. All beams exhibited similar stiffness until crack initiation because the whole uncracked cross-sectional area for all specimens was available for moment resistance. Once the cracks were initiated, the CFRP-strengthened beams exhibited higher stiffness compared with CBs (refer to Figs. 7–9). For illustration, the CFRP-strengthened specimens demonstrated 42% higher stiffness during this loading stage at 28 days, and 52% in specimens exposed to saline water for 360 days [Fig. 8(f)]. The second phase of the load–deflection curves was from steel yielding until the failure of the beam specimens. The stiffness of the CFRP beams in this region was also up to 40% higher than their CBs. This range of increased stiffness after crack initiation was observed in all exposed samples compared with their counterpart CBs.

The yielding of the main reinforcement was initiated at much higher loads in CFRP-strengthened specimens than the CBs (Table 2). The CB specimens tested at 28 days had an average yield and failure load of 89 and 90 kN, respectively. The CFRP-strengthened beams exhibited an average yield and failure load of 124 and 150 kN,

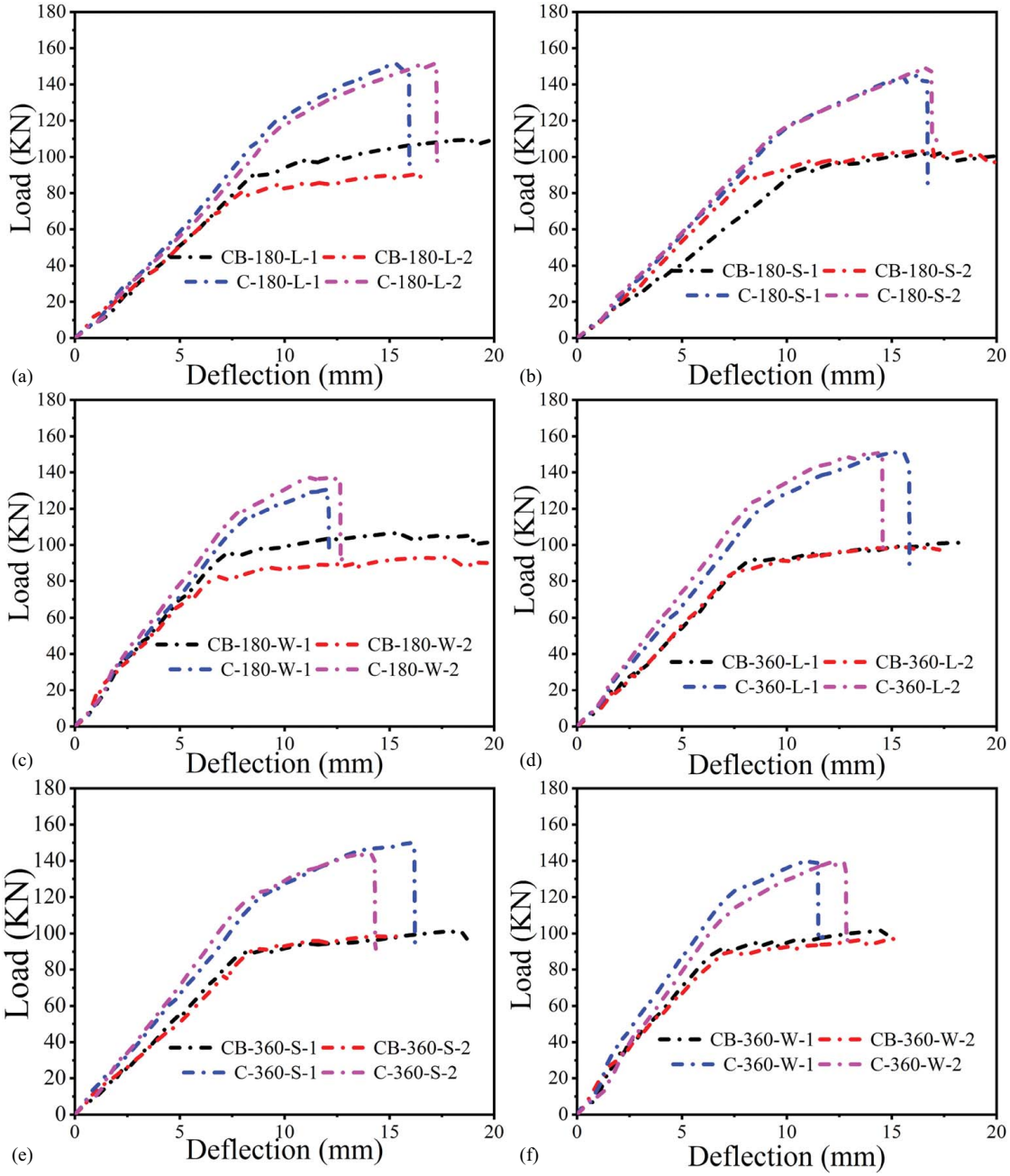

Fig. 8. Midspan load–deflection curves of the control beam (CB) and carbon fiber-reinforced polymer (CFPR)-strengthened specimens exposed to laboratory, sunlight, and saline water conditions for 180 (a–c) and 360 (d–f) days, respectively.

respectively, which indicates an increase of about 40% in the yield load and 67% in the ultimate load-carrying capacity.

At 180 days of laboratory, saline water, and sunlight conditioning, the average yield loads for CB were 86, 89, and 92 kN, respectively, and they failed at 99, 102, and 103 kN, respectively. Moreover, the CFRP-strengthened specimens had an average yield load of 120, 117, and 115 kN, respectively. This shows an average increase of 40%, 32%, and 25% from their respective CB samples exposed to the laboratory and saline water, respectively. The ultimate loads were 150, 134, and 1,146 kN at 180 days for the laboratory, saline water, and sunlight exposure, respectively. This is an average increase of 53%, 32%, and 41% from their counterpart CBs, respectively. A decrease in the percentage enhancement in yield and failure loads occurred at 180 days compared to that of 28 days. This could be due to the loss of bond strength of the epoxy during the first six months. Moreover, CB specimens at 180 days exhibited higher ultimate strength compared with that at 28 days for the control specimens due to the continuous hydration of unhydrated cement, which also lowered the percentage of the strength enhancement for CFRP-strengthened specimens.

Figs. 8(d–f) shows the effects of three exposure at 360 days. The average yield loads of CBs were 89, 91, and 91 kN, whereas the failure loads were 101, 99, and 99 kN for the laboratory, saline water, and sunlight exposure, respectively. The CFRP specimens began yielding at 122, 120, and 119 kN and at ultimate loads of 150, 141, and 147 kN under laboratory, saline water, and sunlight exposure, respectively. Thus, increases occurred of 38%, 33%, and 30% in the yield loads over their CBs, laboratory, saline water, and sunlight exposure, respectively. In addition, the average increases in the ultimate load-carrying capacity were 49%, 42%, and 48%,

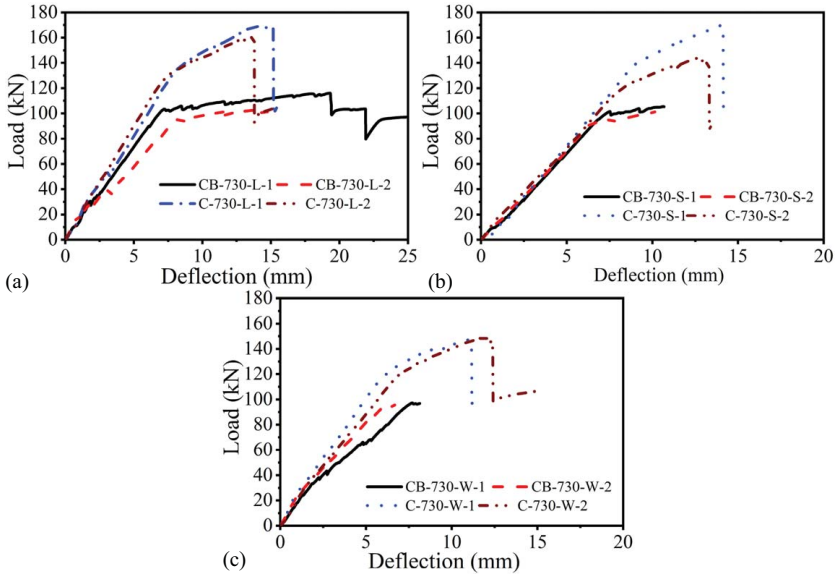

Fig. 9. Midspan load–deflection of the control beam (CB) and carbon fiber-reinforced polymer (CFRP) beams at 730 days of (a) laboratory; (b) sunlight; and (c) saline water exposure.

respectively. Fig. 9 illustrates the behavior of the specimens tested after 730 days (two years) of exposure. The yielding of steel for CBs initiated at 99, 96, and 97 kN, whereas for CFRP beams, it was initiated at 121, 137, and 129 kN, respectively, for laboratory, saline water, and sunlight exposure. The ultimate load capacity in the CBs after 730 days was 109, 96, and 103 kN, respectively, for the laboratory, saline water, and sunlight exposure. For the CFRP, the average ultimate loads were 148, 164, and 156 kN for the laboratory, saline water, and sunlight exposure, respectively. The increase in the yield load in the CFRP-strengthened specimens was 22%, 42%, and 32% for the laboratory, saline water, and sunlight exposure, and the ultimate load was increased by 36%, 71%, and 51% compared with the CBs exposed to similar conditions. Thus, the sunlight and saline water exposure had no significant effect on the ultimate strength of the CFRP-strengthened RC beam, until 730 days. The load–deflection curves demonstrated no loss in beam stiffness, yield loads, or ultimate loads. In addition, these curves followed a behavior similar to those tested at 28 days or to those tested under laboratory conditions.

A decline in strength of the CFRP-strengthened specimens occurred at 180 days under saline water and sunlight exposure. Laboratory exposure demonstrated no loss in strength over the two years. The strength loss under outdoor exposure at 180 days was regained at 360 and 730 days of exposure. Such behavior has already been documented, where an initial loss in strength occurs, and then the strength of the CFRP-based specimens was enhanced (El-Hawary et al. 1998; Choi et al. 2012; Tatar and Hamilton 2016c). El-Hawary et al. (2000) observed an initial drop in the strength of the cylindrical samples strengthened with three different commercial epoxies and exposed to the harsh outdoor climate of the Arabian Gulf coastal region. The strength of the specimens was regained six months after the previous testing, which followed another drop in strength after six months. This suggests that epoxy-based materials are affected by the seasonal environment and fluctuations in temperature and humidity. The strength could be affected by the weather of the previous six months to one year before the testing dates. In this study, the samples were strengthened in April when the temperature is quite moderate in the Gulf region. The 180-day testing was conducted in the month of October. During this exposure period, the specimens were exposed to the weather of extreme temperatures of (≥50°C) and 80% to 100% RH, which is encountered in the months of June to September under sunlight and saline water exposure. The temperature on the concrete surface could have reached above T_g, which softens the epoxy. The temperatures remained in the proximity of 40°C to 50°C until October. This does not allow sufficient time for the softened epoxy to cure before the testing. Hence, lower strengths were observed in the samples tested at 180 days, and most of the failures were adhesive (i.e., the debonding of sheets with traces of concrete). In the case of specimen tests after 360 days (one year) of exposure, the specimens had already weathered the hot temperature cycle, where the softening of epoxy causes more reaction sites and cross-linking inside the epoxy matrix. Then, the winter temperatures allowed proper curing and hardening again. This increases the bond strength between the epoxy and concrete substrate. Hence, a regain in strength in all samples was observed.

No clear patterns were found for the ultimate strength differences between the CFRP-strengthened and CB specimens, and either no loss or a slight increase in the ultimate load capacity after exposure to sunlight and saline water was observed. For example, 71% and 51% increases in the load capacity of CFRP beams after 730 days occurred for saline water and sunlight exposure, respectively, compared with the counterpart CBs, whereas the increases were only 32% and 41% at 180 days, respectively. The increase in strength over prolonged exposure could be due to polymeric cross-linking in epoxy composites. This phenomenon is facilitated at higher temperatures and forms complex interactions in the epoxy matrix. Hence, it improves the interfacial bonding between the CFRP laminate and concrete (Choi et al. 2012; Al-Tamimi et al. 2015). A similar observation of enhancement in bond strength between the CFRP and concrete prisms, when exposed to the sunlight and saline water, was reported by Al-Tamimi et al. (2015). Cromwell et al. (2011) reported similar results in which, under hygrothermal exposure, the strength of the beams strengthened in flexure was enhanced. It was argued that additional post-curing at higher temperatures regenerates the reaction site; hence, adhesive bonds could increase. In addition, some particles of cement always remain unhydrated at the initial curing, and the hydration is accelerated based on the availability of moisture over time, enhancing the concrete strength. Hence, an increase in concrete strength

could also be a reason for the increase in the ultimate strength of the strengthened beam.

Table 2 presents the ductility indices for CB and CFRP-strengthened specimens. The CB specimens had much higher ductility under all exposure conditions and testing durations. However, the CFRP specimens lost ductility at failure due to higher attained loads with lesser deflections. The $\mu_{\Delta y}$ values for CB over all exposure types were between 1.23 and 3.95. The lower value of 1.23 is only observed in samples where loading was stopped after yielding. This was to keep the beam integrity intact for another ongoing strengthening project. The specimens that were loaded until concrete crushing had values of between 2.06 and 3.93. That is an increase of up to 300% of deflection at failure when compared with that at yielding. For the CFRP-strengthened specimens, the $\mu_{\Delta y}$ values were between 1.52 and 1.95. Thus, the ductility loss was up to 159% in the CFRP specimens compared with CBs. Again, no clear pattern in the $\mu_{\Delta y}$ values was observed for the strengthened specimens after exposure to three different environments over two years. The samples tested after one year under laboratory, saline water, and sunlight exposure had an average value of 1.76, 1.71, and 1.76, respectively. After two years, the values were 1.75, 1.65, and 1.57, respectively. The highest value of 1.76 was observed for the sunlight-exposed samples. The slight decrease in the ductility in the samples at 730 days compared with 360 days was due to the gain in the ultimate load capacity.

The $\mu_{\Delta u}$ values for CB were from 1.03 to 1.70, which means up to 70% higher deflection at the failure load than at the ultimate load was observed. Lower values of $\mu_{\Delta u}$ for CB specimens are due to the flat load–deflection curves after yielding until failure. Hence, the ultimate loads are quasi-similar to the failure loads. The CFRP specimens had $\mu_{\Delta u}$ values quite close to 1 because the ultimate and failure loads occurred almost at the same deflections as for those specimens. This loss in ductility in strengthened samples remained in the same range for all exposure times. The exposure to harsh climatic conditions exhibited no visible trend (Table 2).

Strain Response Curves

Fig. 10 depicts the load versus strains of flexural reinforcement and concrete in compression at the midspan beams tested at 28 days. Figs. 11–13 list the strains for the specimens conditioned under laboratory, saline water, and sunlight exposure after 180, 360, and 730 days, respectively. The curve for one sample from each exposure and time is presented.

The steel yielding strain as per the manufacturer was 0.0027 mm/mm. It is evident from Figs. 10 to 13 that the steel yielded in the CB at a load of between 86 and 92 kN and reached an ultimate strain of 0.0027. The CB specimens failed in flexure by steel yielding, followed by concrete crushing at the ultimate strains of up to 0.003 mm/mm. In some specimens, the strain gauges malfunctioned, and the complete behavior until failure was not observed at those locations. After yielding, the strain gauges recorded smaller values than those observed at yielding. For example, the steel strain gauges of the CB-360-L-1 and CB 360-S-1 specimens indicated unexpected behavior during loading. In the CFRP specimens, the slopes of the load versus the steel strain curves were higher than those of the CBs. After steel yielding, the crushing of concrete was not initiated. Instead, concrete kept taking strain; however, the slope of the curves was reduced (Figs. 10–13). Then, at the failure load, the concrete was crushed immediately due to the debonding of the CFRP sheet. Thus, the failure strains of the concrete in the strengthened specimens were also reduced compared with those of the CBs. This behavior remained similar in all specimens under the three exposure types and times.

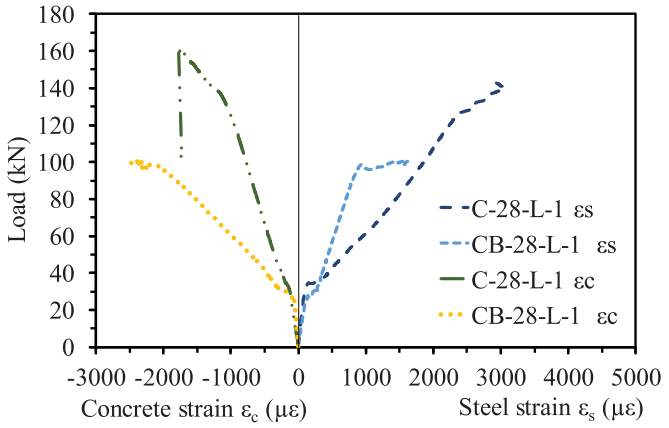

Fig. 10. Strain of the steel reinforcement and concrete in specimens tested at 28 days.

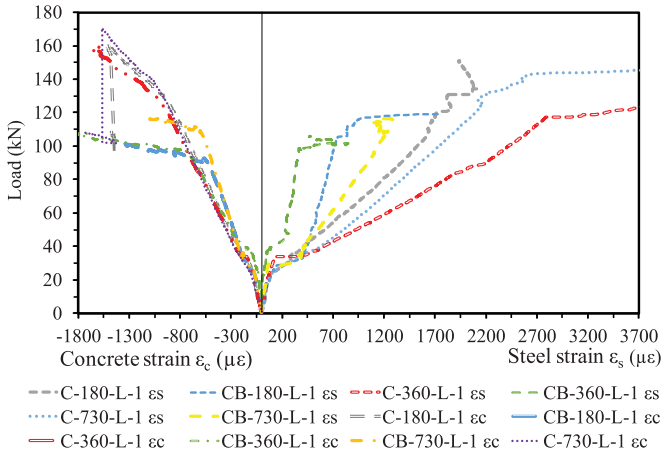

Fig. 11. Strain of the flexural reinforcement and top surface concrete at midspan of the beams placed under laboratory environment for 180, 360, and 730 days.

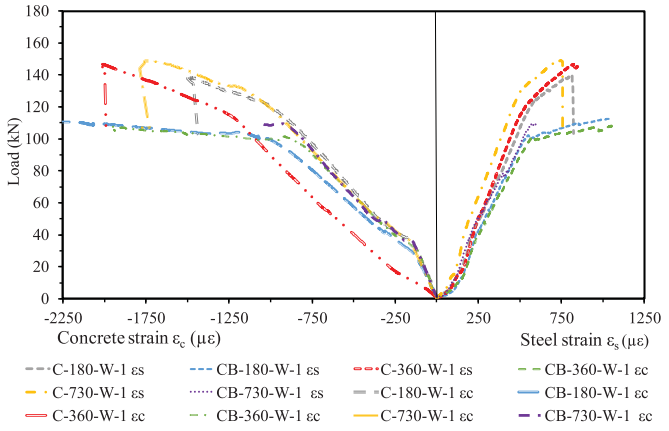

Fig. 12. Strain of the flexural reinforcement and top surface concrete at the midspan for the specimens placed under saline water for 180, 360, and 730 days.

Fig. 11 demonstrates the effects of laboratory exposure on the strain behavior of the CFRPs and CBs over time. From the samples placed in the laboratory, the steel strain value at 180 days was smaller than those at 360 and 730 days of exposure, respectively.

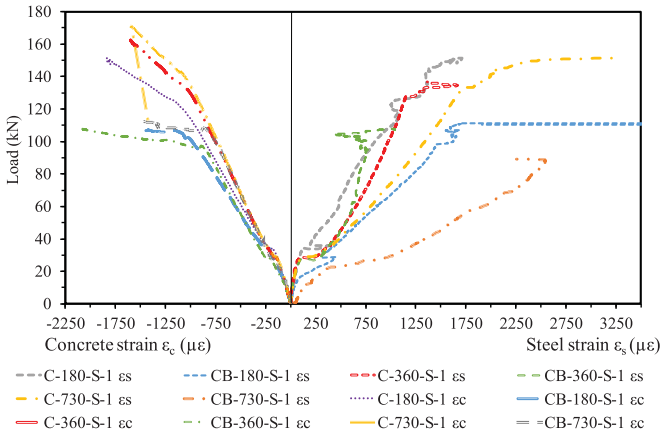

Fig. 13. Strain of the flexural reinforcement and top face concrete at the midspan of the specimens placed under direct sunlight for 180, 360, and 730 days.

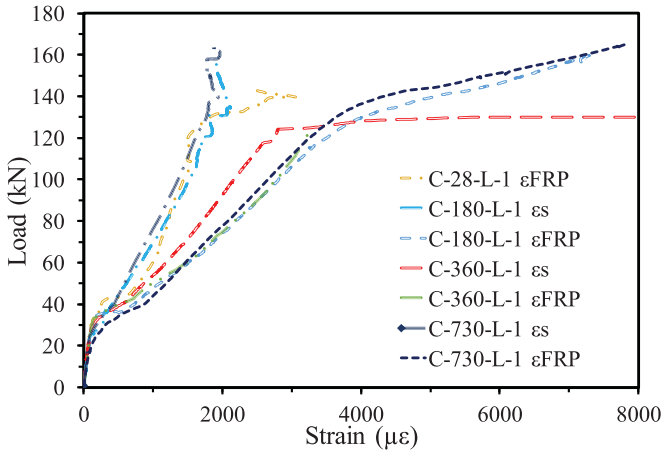

Fig. 14. Strain values in the main reinforcement and carbon fiber-reinforced polymer (CFRP) laminates placed under laboratory environment for 180, 360, and 730 days.

The slope of the curve (stiffness) was slightly decreased for the 360-day specimens compared with the 180-day specimens. However, the specimens tested at 730 days again had a higher slope than the 180-day samples. Fig. 12 reveals that saline water exposure had no influence on the strain of flexure reinforcement over time (up to two years). The curve for the CFRP samples at 730 days exhibited higher stiffness than did those samples tested at 180 and 360 days. This is another indication that CFRP sheets and epoxy adhesives were not affected by saline water exposure. Instead, it had a positive effect on the durability of the strengthened concrete beams. The load versus the strain curves of the concrete in compression also exhibited similar behavior at up to 730 days for samples placed in the laboratory. The yield and ultimate crushing values were in close range for all samples at up to two years of exposure. In the case of saline water exposure, the concrete behavior was slightly different, according to the exposure time. Higher strains were achieved in the beams tested at 360 and 730 days compared with 180 days, before the crushing of the concrete. Fig. 13 presents the effects of sunlight exposure over 180, 360, and 730 days of exposure. Similarly, the exposure does not affect the concrete strains and beam stiffness. Instead, slightly higher stiffness with time was observed in the beams tested at 360 and 730 days compared with those at 180 days.

Fig. 14 compares the strains in the primary reinforcement and CFRP laminates in the specimens test at 28 days and the specimens tested under laboratory exposure at 180, 360, and 730 days. Figs. 15 and 16 present the values for specimens under the saline water and sunlight exposure for 180, 360, and 730 days, respectively. Strains in steel and CFRP laminates were similar until the first crack appeared in the strengthened beams. After cracks appeared, the strain in the CFRP laminates increased compared with the steel strain. This is attributed to the stress transfer to these laminates, as the concrete in the tensile zone seized to take any further stress after cracking. The strain in the laminates was also much higher compared with the steel strain, which is because these laminates are placed farther in depth from the neutral axis than the steel rebar, which generates higher tensile moments in the laminates. Up to 3 to 4 times higher strain values were endured by the CFRP laminates than the steel rebar at failure. Figs. 15 and 16 reveal that this behavior was similar in all the samples tested after each exposure period. For example, the exposure for two years had a negligible effect on the behavior of the CFRP laminates, strengthened beams, and bond between the concrete and laminates.

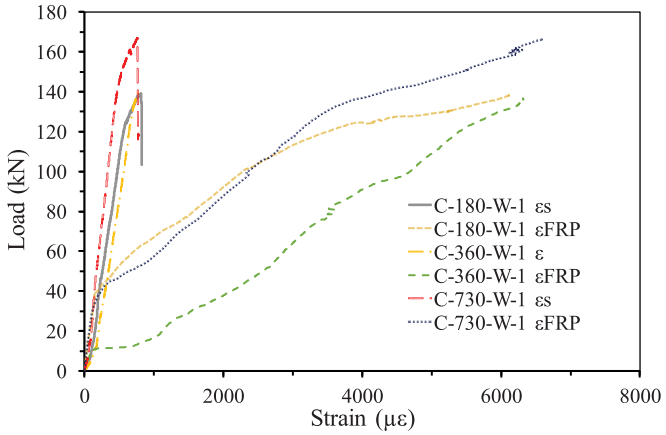

Fig. 15. Strain values in the main reinforcement and carbon fiber-reinforced polymer (CFRP) laminates saline water for 180, 360, and 730 days.

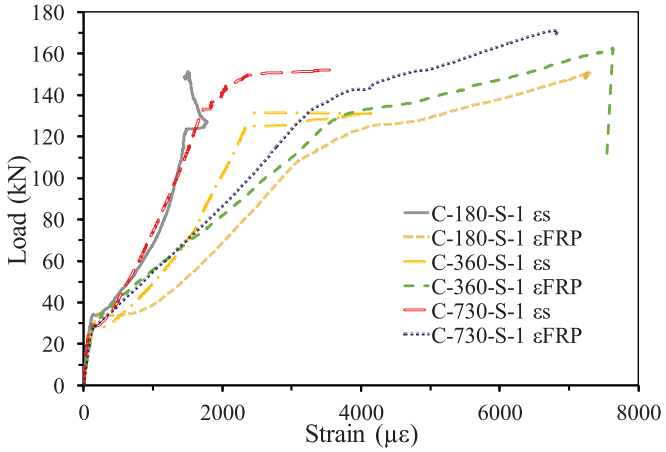

Fig. 16. Strain values in the main reinforcement and carbon fiber-reinforced polymer (CFRP) laminates placed under the sunlight exposure for 180, 360, and 730 days.

Degradation Indices

The degradation indices for the CFRP-strengthened beams after each exposure are graphically presented in Fig. 17. Table 3 lists the average values of the environmental degradation indices over two CFRP-strengthened specimens for each category. The severe climatic conditions could affect the CFRP-strengthened RC beams on three levels. The first is the degradation of RC beams caused by the corrosion of the steel reinforcement or by the chemical attacks on the concrete matrix. The second is the bond degradation between the CFRP laminates and concrete due to the damage caused to the epoxy matrix, and the third is damage to the CFRP sheets and its fibers.

In the cases mentioned, the residual strength of the CFRP-strengthened beams is reduced compared with the unexposed samples. The values of *ESR*, and the ratios, R_n, R_b, and R_{b28} should be less than 1.0. The *ESR* values were 0.96, 0.98, and 1.05 for sunlight exposure and 0.88, 0.94, and 1.11 for saline water exposure after 6, 12, and 24 months, respectively. The flexural strength reduction factor R_n for saline water exposure was a minimum of 0.86 at 180 days, whereas after 730 days, it increased to 1.25. For sunlight exposure, R_n was 0.92, 0.99, and 1.11 after 180, 360, and 730 days, respectively. The bond strength reduction factor R_b was 0.61, 0.84, and 1.71 for saline water exposure at 180, 360, and 730 days, respectively. Under sunlight exposure, R_b was 0.81, 0.97, and 1.34, respectively. For the first 180 days, the strength was reduced compared with 28 days; however, it was recovered after 360 and 730 days (Fig. 17). The specimens tested at 730 days indicated higher strength compared with the samples tested at 28 days. Most degradation index values were closer to 1, indicating a minor loss or some gain in strength.

This reveals that, with age, the epoxy-based strengthening system matures by forming more cross-links in the epoxy matrix; hence, a slightly higher mechanical performance and durability is possible for the strengthened specimens. This observation has also been made by other researchers (Grace and Singh 2005; Choi et al. 2012; Al-Tamimi et al. 2015). When the climate temperature reaches close to T_g, the epoxy materials soften, which reactivates the cross-linking in the matrix. If allowed to cure and hardened again, the material could achieve higher strength (Nogueira et al. 2001; Choi and Douglas 2010).

Fig. 17 indicates that some loss in strength occurs in the samples exposed to both exposure types for 180 days. However, the strength was regained after 360 and 730 days, especially in the saline water exposure. This behavior of the epoxy-based strengthening systems

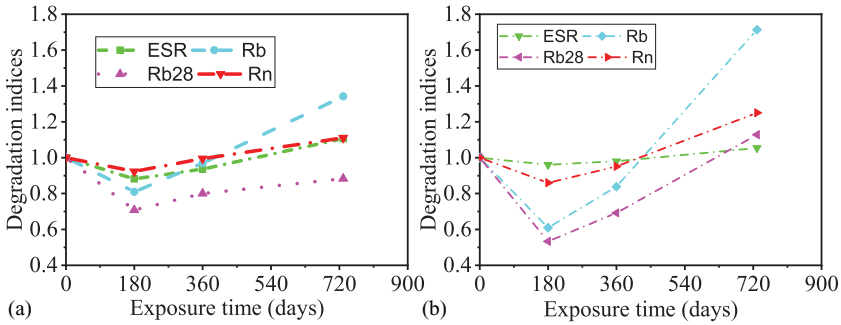

Fig. 17. Degradation indices for carbon fiber-reinforcement polymer (CFRP) under (a) sunlight; and (b) saline water, respectively, after exposure for 180, 365, and 730 days.

Table 3. Average values of different environmental degradation indices for carbon fiber-reinforced polymer (CFRP)-strengthened beams over 180, 360, and 730 days

Exposure time	Conditions	Str. Type	Ultimate loads P_u (kN)	Degradation indices					
				LSR	ESR	ESR/LSR	R_n	R_b	R_{b28}
28 days	Lab	Control	90	—	—	—	—	—	—
		CFRP	150	1.67	—	—	—	—	—
6 months	Lab	Control	99	—	—	—	—	—	—
		CFRP	152	1.53	—	—	—	—	—
	Saline	Control	102	—	—	—	—	—	—
		CFRP	134	—	0.88	0.58	0.86	0.61	0.53
	Sun	Control	103	—	—	—	—	—	—
		CFRP	146	—	0.96	0.63	0.92	0.81	0.71
12 months	Lab	Control	101	—	—	—	—	—	—
		CFRP	150	1.49	—	—	—	—	—
	Saline	Control	99	—	—	—	—	—	—
		CFRP	141	—	0.94	0.63	0.95	0.84	0.69
	Sun	Control	99	—	—	—	—	—	—
		CFRP	147	—	0.98	0.66	0.99	0.97	0.80
24 months	Lab	Control	109	—	—	—	—	—	—
		CFRP	148	1.36	—	—	—	—	—
	Saline	Control	96	—	—	—	—	—	—
		CFRP	164	—	1.11	0.81	1.25	1.71	1.13
	Sun	Control	103	—	—	—	—	—	—
		CFRP	156	—	1.05	0.77	1.11	1.34	0.88

Table 4. Recommendations for environmental strength reduction factors

Standards/This study	Exposure	Reduction factor for CFRP
ACI 440.2R-17	Interior	0.95
	Exterior	0.85
Recommended bond capacity (R_b)	Saline water	0.60
	Sunlight	0.8
Recommended flexural strength (R_n)	Saline water	0.85
	Sunlight	0.95

has already been reported under brackish water and sunlight exposure (Choi et al. 2012; Al-Tamimi et al. 2015; Tatar and Hamilton 2016c). The barnacles formed due to the lengthy immersion under brackish water also contribute to the strength of the whole member. Moreover, they protect the concrete and strengthening systems from deterioration by forming a protective layer (Choi et al. 2012; Al-Tamimi et al. 2015; Al Nuaimi et al. 2020). In addition, the type of epoxy, mixing ratio of its parts, and applied amount significantly affect the durability and strength performance of strengthened concrete specimens (Toutanji and Gómez 1997; Choi et al. 2012; Al-Tamimi et al. 2015). For detailed chemistry involved in the cross-linking and creation of activation sites, readers are referred to the works of Liu et al. (2019), Choi et al. (2012), and Al-Tamimi et al. (2015).

The strength-reduction factors (C_E), which are employed during the analysis and design of CFRP-strengthened RC beams, are presented in Table 4 in comparison with those recommended by ACI 440.2R-17 (ACI 2017), which provides C_E values for interior and exterior exposure for conventional CFRP-strengthened members at 0.95 and 0.85, respectively. Based on the results of this study, we present a comparison between the recommended C_E for the CFRP-strengthened RC beams under saline water and sunlight exposure conditions. The reduction factors for bond strength R_b and flexural strength R_n were 0.60 and 0.85 for saline water, respectively, and 0.80 and 0.95 for sunlight exposure, respectively. Grace and Singh (2005) found similar values for CFRP sheets under saline and 100% humidity exposure. In contrast, Tatar and Hamilton (2016a) recommended a bond durability factor of 0.60 after applying accelerated hydrothermal conditioning to the CFRP-strengthened systems.

Except for one odd value of R_{b28} of 0.53 for saline water exposure, based on the results of this study, the C_E recommended values by the ACI 440.2R-17 (ACI 2017) guidelines are reasonable and logical. These bond degradation factors are estimated based on the strengthening system without any anchorage of CFRP laminates to the web of the beam specimens. Environmental reduction factors recommended in this study could be important for the design and analysis of RC beams strengthened with CFRP, especially when the durability of strengthening systems under harsh climates is under consideration.

Because the behavior of the two tested specimens at each exposure type was very similar, the effects of the applied environment were properly covered. However, because the number of samples for each category was limited to only two, a complete statistical analysis to enhance the confidence in the durability behavior of the CFRP systems was not possible. Furthermore, the study was limited to two years of exposure, which is a short period considering the service life of a repaired RC structure. That is why a prolonged study exceeding two years is recommended in which a comprehensive study on cracking, stiffness, and failure modes could be conducted to increase the database on the durability aspect of strengthening systems.

Conclusions

The durability performance of RC beams strengthened with CFRP composites was evaluated under the harsh environmental conditions of sunlight and saline water after an exposure period of 6, 12, and 24 months. The results of the four-point bending tests after each exposure were compared with the specimens tested at 28 days, to the unstrengthened control specimens with similar exposure, and to the strengthened samples placed in the laboratory environment for the same length of time.

The following are the main observations and conclusions:

- A slight loss in strength was observed in specimens tested at 180 days, which was regained in specimens tested at 360 and 730 days. At 730 days, the strength was higher than those samples tested at 28 days.
- It was observed that even after constant exposure to high tropical temperatures, which results in a concrete surface temperature near the glass transition temperature of the epoxy, the CFRP-strengthened specimens exhibited marginal or, in some cases, no loss in strength.
- The failure modes were changed from cohesive to adhesive in saline water exposure even after 180 days, indicating that the epoxy bond becomes a critical aspect in hygrothermal exposure. The sunlight exposure exhibited no influence on the failure mode.
- Exposure to 3.5% NaCl solution and direct sunlight for 6, 12, and 24 months resulted in no significant effect on beam stiffness in the CFRP-strengthened specimens. The carbon fiber in the CFRP laminates also demonstrated no sign of deterioration.
- The bond strength reduction factors of CFRP-strengthened members exposed to saline water and sunlight are recommended at 0.6 and 0.80, respectively. The flexure strength reduction factor was 0.85 and 0.95 for saline water and sunlight exposure, respectively. For saline water exposure, the value of the recommended reduction factor was smaller (conservative) than that recommended by ACI 440.2R-17 (ACI 2017). However, for sunlight exposure, the environmental reduction factors provided by ACI 440.2R-17 (ACI 2017) are reasonable for CFRP-strengthened systems for such harsh outdoor climate exposure.
- Because the provided recommendations are based on the outcome of a two-year study, it is recommended to test the strengthening systems for prolonged exposure so that the confidence in their durability can be enhanced.

Data Availability Statement

The generated data during this study are available from the corresponding author by request (stress–strain data, load–deflection data, proposed degradation data, and crack initiation data).

Acknowledgments

The funding for this research was provided by the National Priorities Research Program of the Qatar National Research Fund (a member of the Qatar Foundation) under award no. NPRP 8-418-2-175. The statements made herein are solely the responsibility of the authors and do not necessarily reflect the opinions of the Sponsor.

References

Abbas, B. M. M. 2010. "Durability of CFRP-concrete bond under sustained load in harsh environment." Ph.D. thesis, Dept. of Civil Engineering, Monash Univ.

ACI (American Concrete Institute). 2014. *Building code requirement for structural concrete*. ACI 318-14. Farmington Hills, MI: ACI.
ACI (American Concrete Institute). 2017. *Guide for the design and construction of externally bonded FRP systems for strengthening concrete structures*. ACI 440.2R-17. Farmington Hills, MI: ACI.
Al Azzawi, M., P. Hopkins, J. Ross, G. Mullins, and R. Sen. 2018. "Carbon fiber-reinforced polymer concrete masonry unit bond after 20 years of outdoor exposure." *ACI Struct. J.* 115 (4): 971–982. https://doi.org/10.14359/51702226.
Al Nuaimi, N., M. G. Sohail, R. A. Hawileh, J. A. Abdalla, and K. Douier. 2020. "Durability of reinforced concrete beams strengthened by galvanized steel mesh-epoxy systems under harsh environmental conditions." *Compos. Struct.* 249: 112547. https://doi.org/10.1016/j.compstruct.2020.112547.
Al-Tamimi, A. K., R. Hawileh, J. Abdalla, and H. A. Rasheed. 2011. "Effects of ratio of CFRP plate length to shear span and end anchorage on flexural behavior of SCC RC beams." *J. Compos. Constr.* 15 (6): 908–919. https://doi.org/10.1061/(ASCE)CC.1943-5614.0000221.
Al-Tamimi, A. K., R. A. Hawileh, J. A. Abdalla, H. A. Rasheed, and R. Al-Mahaidi. 2015. "Durability of the bond between CFRP plates and concrete exposed to harsh environments." *J. Mater. Civ. Eng.* 27 (9): 04014252. https://doi.org/10.1061/(ASCE)MT.1943-5533.0001226.
ASTM. 2012. *Standard test method for flexural performance of fiber-reinforced concrete (using beam with third-point loading)*. ASTM C1609/C1609M-12. West Conshohocken, PA: ASTM.
ASTM. 2015. *Standard test method for slump of hydraulic-cement concrete*. ASTM C143/C143M-15a. West Conshohocken, PA: ASTM.
ASTM. 2016. *Standard specification for deformed and plain carbon-steel bars for concrete reinforcement*. ASTM A615/A615M-16. West Conshohocken, PA: ASTM.
ASTM. 2017. *Standard test method for compressive strength of cylindrical concrete specimens*. ASTM C39/C39M-17. West Conshohocken, PA: ASTM.
Bahn, B. Y., and R. S. Harichandran. 2008. "Flexural behavior of reinforced concrete beams strengthened with CFRP sheets and epoxy mortar." *J. Compos. Constr.* 12 (4): 387–395. https://doi.org/10.1061/(ASCE)1090-0268(2008)12:4(387).
Bakis, C. E., L. C. Bank, V. L. Brown, E. Cosenza, J. F. Davalos, J. J. Lesko, A. Machida, S. H. Rizkalla, and T. C. Triantafillou. 2002. "Fiber-reinforced polymer composites for construction—State-of-the-art review." *J. Compos. Constr.* 6 (2): 73–87. https://doi.org/10.1061/(ASCE)1090-0268(2002)6:2(73).
Cabral-Fonseca, S., J. P. Nunes, M. P. Rodrigues, and M. I. Eusébio. 2011. "Durability of carbon fibre reinforced polymer laminates used to reinforced concrete structures." *Sci. Eng. Compos. Mater.* 18 (4): 201–207. https://doi.org/10.1515/SECM.2011.041.
Choi, S., and E. P. Douglas. 2010. "Complex hygrothermal effects on the glass transition of an epoxy-amine thermoset." *ACS Appl. Mater. Interfaces* 2 (3): 934–941. https://doi.org/10.1021/am9009346.
Choi, S., A. L. Gartner, N. Van Etten, H. R. Hamilton, and E. P. Douglas. 2012. "Durability of concrete beams externally reinforced with CFRP composites exposed to various environments." *J. Compos. Constr.* 16 (1): 10–20. https://doi.org/10.1061/(ASCE)CC.1943-5614.0000233.
Choobbor, S. S., R. A. Hawileh, A. Abu-Obeidah, and J. A. Abdalla. 2019. "Performance of hybrid carbon and basalt FRP sheets in strengthening concrete beams in flexure." *Compos. Struct.* 227: 111337. https://doi.org/10.1016/j.compstruct.2019.111337.
Chotickai, P., and S. Somana. 2018. "Performance of CFRP-strengthened concrete beams after exposure to wet/dry cycles." *J. Compos. Constr.* 22 (6): 04018053. https://doi.org/10.1061/(ASCE)CC.1943-5614.0000895.
Cromwell, J. R., K. A. Harries, and B. M. Shahrooz. 2011. "Environmental durability of externally bonded FRP materials intended for repair of concrete structures." *Constr. Build. Mater.* 25 (5): 2528–2539. https://doi.org/10.1016/j.conbuildmat.2010.11.096.
Dolan, C. W., J. Tanner, D. Mukai, H. R. Hamilton, and E. Douglas. 2009. *Design guidelines for durability of bonded CFRP repair/strengthening of concrete beams*. National Cooperative Highway Research Program (NCHRP) Web-Only Document 155. Washington, DC: National Academies of Sciences, Engineering, and Medicine.
El-Hawary, M., H. Al-Khaiat, and S. Fereig. 1998. "Effect of sea water on epoxy-repaired concrete." *Cem. Concr. Compos.* 20 (1): 41–52. https://doi.org/10.1016/S0958-9465(97)00074-7.
El-Hawary, M., H. Al-Khaiat, and S. Fereig. 2000. "Performance of epoxy-repaired concrete in a marine environment." *Cem. Concr. Res.* 30 (2): 259–266. https://doi.org/10.1016/S0008-8846(99)00242-2.
Gamage, J. C., M. B. Wong, and R. Al-Mahaidi. 2005. "Performance of CFRP strengthened concrete members under elevated temperature." In *Int. Symp. Bond Behaviour of FRP in Structures*, 113–118. Hong Kong: International Institute for FRP in Construction.
Grace, N. F., and S. B. Singh. 2005. "Durability evaluation of carbon fiber-reinforced polymer strengthened concrete beams: Experimental study and design." *ACI Struct. J.* 102 (1): 40–53.
Hanna, S., and R. Jones. 1997. "Composite wraps for ageing infrastructure: Concrete columns." *Compos. Struct.* 38 (1–4): 57–64. https://doi.org/10.1016/S0263-8223(97)00041-X.
Hawileh, R. A., J. A. Abdalla, W. Nawaz, R. Muwafi, A. Alzeer, and A. Faridi. 2014. "Strengthening reinforced concrete beams in flexure using hardwire steel fiber sheets." In *Proc., 7th Int. Conf. on FRP Composites in Civil Engineering*. Kingston, Ontario: International Institute for FRP in Construction.
Hawileh, R., A. K. Al-Tamimi, J. A. Abdalla, and M. H. Wehbi. 2011. "Retrofitting pre-cracked RC beams using CFRP and epoxy injections." In: *Composite science and technology*, edited by S. M. Sapuan, F. Mustapha, D. L. Majid, Z. Leman, A. H. M. Ariff, M. K. A. Ariffin, M. Y. M. Zuhri, M. R. Ishak, and J. Sahari, 692–696. Zurich, Switzerland: Trans Tech Publications.
Helbling, C., M. Abanilla, L. Lee, and V. M. Karbhari. 2006. "Issues of variability and durability under synergistic exposure conditions related to advanced polymer composites in the civil infrastructure." *Composites, Part A* 37 (8): 1102–1110. https://doi.org/10.1016/j.compositesa.2005.05.039.
Karbhari, V. M. 2003. "Durability of FRP composites for civil infrastructure—Myth, mystery or reality." *Adv. Struct. Eng.* 6 (3): 243–255. https://doi.org/10.1260/136943303322419250.
Karbhari, V. M., J. W. Chin, D. Hunston, B. Benmokrane, T. Juska, R. Morgan, J. J. Lesko, U. Sorathia, and D. Reynaud. 2003. "Durability gap analysis for fiber-reinforced polymer composites in civil infrastructure." *J. Compos. Constr.* 7 (3): 238–247. https://doi.org/10.1061/(ASCE)1090-0268(2003)7:3(238).
Karbhari, V. M., and L. Zhao. 1997. "Issues related to composite plating and environmental exposure effects on composite-concrete interface in external strengthening." *Compos. Struct.* 40 (3–4): 293–304. https://doi.org/10.1016/S0263-8223(98)00031-2.
Li, J., R. J. Gravina, S. T. Smith, and P. Visintin. 2020. "Bond strength and bond stress-slip analysis of FRP bar to concrete incorporating environmental durability." *Constr. Build. Mater.* 261: 119860. https://doi.org/10.1016/j.conbuildmat.2020.119860.
Li, J., J. Xie, F. Liu, and Z. Lu. 2019. "A critical review and assessment for FRP-concrete bond systems with epoxy resin exposed to chloride environments." *Compos. Struct.* 229: 111372. https://doi.org/10.1016/j.compstruct.2019.111372.
Liu, S., Y. Pan, H. Li, and G. Xian. 2019. "Durability of the bond between CFRP and concrete exposed to thermal cycles." *Materials* 12 (3): 515. https://doi.org/10.3390/ma12030515.
Micelli, F., R. Mazzotta, M. Leone, and M. A. Aiello. 2015. "Review study on the durability of FRP-confined concrete." *J. Compos. Constr.* 19 (3): 04014056. https://doi.org/10.1061/(ASCE)CC.1943-5614.0000520.
Myers, J. J., S. S. Murthy, and F. Micelli. 2001. "Effect of combined environmental cycles on the bond of FRP sheets to concrete." In: *Proc., Composite in Construction, Int. Conf.*, edited by J. Figueiras, L. Juvandes, R. Faria, A. Torres Marques, A. Ferreira, J. Barros, and J. Appleton, 339–344. Lisse, UK: Balkema.
Naser, M. Z., R. A. Hawileh, and J. A. Abdalla. 2019. "Fiber-reinforced polymer composites in strengthening reinforced concrete structures: A critical review." *Eng. Struct.* 198: 109542. https://doi.org/10.1016/j.engstruct.2019.109542.
Naser, M. Z., R. A. Hawileh, J. A. Abdalla, and A. Al-Tamimi. 2012. "Bond behavior of CFRP cured laminates: Experimental and numerical

investigation." *J. Eng. Mater. Technol.* 134 (2): 021002. https://doi.org/10.1115/1.4003565.

Nishizaki, I., P. Labossière, and B. Sarsaniuc. 2005. "Durability of CFRP sheet reinforcement through exposure tests." In *7th Int. Symp. on Fiber-Reinforced (FRP) Polymer Reinforcement for Concrete Structures*, 1419–1428. Farmington Hills, MI: American Concrete Institute.

Nogueira, P., C. Ramírez, A. Torres, M. J. Abad, J. Cano, J. López, I. López-Bueno, and L. Barral. 2001. "Effect of water sorption on the structure and mechanical properties of an epoxy resin system." *J. Appl. Polym. Sci.* 80 (1): 71–80. https://doi.org/10.1002/1097-4628(20010404)80:1<71::AID-APP1077>3.0.CO;2-H.

Pan, Y., G. Xian, and M. A. G. Silva. 2015. "Effects of water immersion on the bond behavior between CFRP plates and concrete substrate." *Constr. Build. Mater.* 101: 326–337. https://doi.org/10.1016/j.conbuildmat.2015.10.129.

Salama, A. S. D., R. A. Hawileh, and J. A. Abdalla. 2019. "Performance of externally strengthened RC beams with side-bonded CFRP sheets." *Compos. Struct.* 212: 281–290. https://doi.org/10.1016/j.compstruct.2019.01.045.

Sen, R. 2015. "Developments in the durability of FRP-concrete bond." *Constr. Build. Mater.* 78: 112–125. https://doi.org/10.1016/j.conbuildmat.2014.12.106.

Shehata, E., R. Morphy, and S. Rizkalla. 2011. "Fibre reinforced polymer shear reinforcement for concrete members: Behaviour and design guidelines." *Can. J. Civ. Eng.* 27 (5): 859–872. https://doi.org/10.1139/cjce-27-5-859.

Smith, S., R. Kaul, R. Ravindrarajah, and O. Otoom. 2005. "Durability considerations for FRP- strengthened RC structures in the Australian environment." In *Proc., Australian Structural Engineering Conf. 2005: Structural Engineering - Preserving and Building Into the Future*. Sydney, New South Wales: Engineers Australia.

Tatar, J., and H. R. Hamilton. 2016a. "Implementation of bond durability in the design of flexural members with externally bonded FRP." *J. Compos. Constr.* 20 (3): 04015072. https://doi.org/10.1061/(ASCE)CC.1943-5614.0000636.

Tatar, J., and H. R. Hamilton. 2016b. "Comparison of laboratory and field environmental conditioning on FRP-concrete bond durability." *Constr. Build. Mater.* 122: 525–536. https://doi.org/10.1016/j.conbuildmat.2016.06.074.

Tatar, J., and H. R. Hamilton. 2016c. "Bond durability factor for externally bonded CFRP systems in concrete structures." *J. Compos. Constr.* 20 (1): 04015027. https://doi.org/10.1061/(ASCE)CC.1943-5614.0000587.

Tatar, J., D. Wagner, and H. R. Hamilton. 2016. "Structural testing and dissection of carbon fiber-reinforced polymer-repaired bridge girders taken out of service." *ACI Struct. J.* 113 (6): 1357–1368. https://doi.org/10.14359/51689160.

Toutanji, H. A., and W. Gómez. 1997. "Durability characteristics of concrete beams externally bonded with FRP composite sheets." *Cem. Concr. Compos.* 19 (4): 351–358. https://doi.org/10.1016/S0958-9465(97)00028-0.

V-Wrap™ 700S. 2014. Strengthening solutions V-WrapTM 700S epoxy adhesive. Structural technologies.

V-Wrap™ C200H. 2014. Strengthening solutions V-WrapTM C200H high strength carbon fiber fabric. Structural technologies.